ACS Catalysis

Research Article

pubs.acs.org/acscatalysis

Elucidation and Evolution of the Active Component within Cu/Fe/ZSM-5 for Catalytic Methane Oxidation: From Synthesis to Catalysis

Ceri Hammond,*[,†,⊥] Nikolaos Dimitratos,[†,∥] Robert L. Jenkins,[†] Jose Antonio Lopez-Sanchez,[†,¶] Simon A. Kondrat,[†] Mohd Hasbi ab Rahim,[†] Michael M. Forde,[†] Adam Thetford,[†] Stuart H. Taylor,[†] Henk Hagen,[‡] Eric E. Stangland,[§] Joo H. Kang,[§] Jacob M. Moulijn,[†] David J. Willock,[†] and Graham J. Hutchings*[,†]

[†]Cardiff Catalysis Institute, School of Chemistry, Cardiff University, Main Building, Park Place, Cardiff, CF10 3AT, United Kingdom

[‡]Dow Benelux B.V., Herbert H. Dowweg 5, 4542 NM HOEK, Postbus 48, 4530 AA Terneuzen, The Netherlands

[§]Corporate R&D, The Dow Chemical Company, Midland, Michigan 48674, United States

Supporting Information

ABSTRACT: The development of a catalytic, one-step route for the oxidation of methane to methanol remains one of the greatest challenges within catalysis. Of particular importance is the need to develop an efficient route that proceeds under mild reaction conditions so as to avoid deeper oxidation and the economic limitations of the currently practiced syngas route. Recently, it was demonstrated that a copper- and iron-containing zeolite is an efficient catalyst for such a one-step process. The catalyst in question (Cu−Fe−ZSM-5) is capable of selectively transforming methane to methanol in an aqueous medium with hydrogen peroxide as the terminal oxidant. Nevertheless, despite its high activity and unparalleled methanol selectivity, the origin of its activity and the precise nature of its active species are not yet fully understood. Through a combination of catalytic and spectroscopic studies, we hereby demonstrate that extraframework Fe species are the active component of the catalyst for methane oxidation, although the speciation of these sites from synthesis to catalysis significantly alters the observed activity and selectivity. The analogies and differences between this system and other iron-containing zeolite-catalyzed processes, such as N_2O-mediated benzene hydroxylation, are also considered.

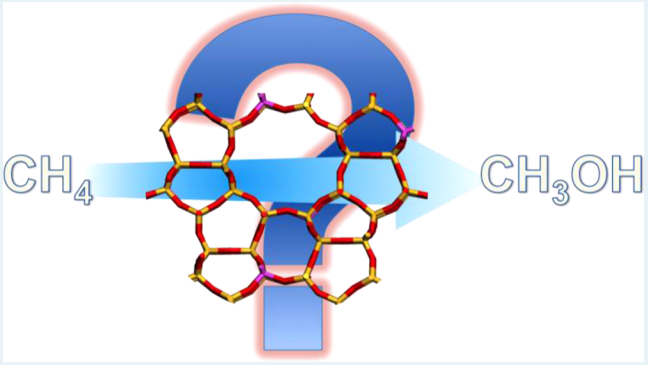

KEYWORDS: *methane oxidation, zeolite catalysis, green chemistry, selective oxidation*

INTRODUCTION

One of the greatest challenges in modern chemistry is the need to develop new, sustainable routes to bulk and commodity chemicals. With this in mind, the valorization of alternative feedstocks to crude oil is of critical importance.[1] Methane, the major constituent of natural gas and other fossil reserves, is a highly abundant and inexpensive source of fuel and chemicals.[2,3] Methane is also the cleanest burning of the fossil fuels, providing a higher energy/CO_2 ratio than other alkanes, and also constitutes around 60% of biogas generated from anaerobic digestion of waste.[4] However, its kinetic inertness (ΔH_{C-H} = 438.8 kJ mol^{-1}) and low reactivity means that current industrial utilization is both indirect and economically intensive. The conversion of methane to methanol, for example, first requires the intermediate manufacture of syngas in an energy- and economically intensive process prior to methanol synthesis in a subsequent step.[5] Significant interest therefore exists in the development of direct routes for the conversion of methane to value-added products. Given its potential as a feedstock for olefin and aromatics production,[6] the selective oxidation of methane to methanol remains one of the most promising routes for methane valorization.

However, competing with the partial oxidation of methane to methanol is the deeper oxidation of methanol. Indeed, the significant increase in reactivity of methanol relative to methane typically results in high selectivities toward carbon oxides, particularly under the conditions historically employed for methane activation (>500 °C) and at high levels of conversion.[1] Thus, the design of catalytic systems capable not only of activating methane but also of doing so under intrinsically mild reaction conditions remains the greatest hurdle toward a selective methane oxidation process.

Recently, the ability of a transition metal-promoted microporous molecular sieve to mediate the selective oxidation of methane to methanol under mild reaction conditions was reported.[7−9] The key to this process is the activation of the

Received: December 10, 2012
Revised: February 5, 2013
Published: February 7, 2013

green oxidant, H_2O_2, and methane by a Cu- and Fe-containing MFI-type zeolite (Cu/Fe/ZSM-5, SiO_2/Al_2O_3 = 30), which results in a novel low-energy pathway to yield the intermediate species methyl hydroperoxide (MeOOH) in a fully closed catalytic cycle. Subsequent conversion of this intermediate yields methanol (MeOH) at high yield and selectivity, although overoxidation to formic acid (HCOOH) and CO_2 is observed at various levels of selectivity. The developed system was found not only to be over 3 orders of magnitude more active than any previously reported for methane oxidation, but also afforded unparalleled selectivity to methanol (>90%) under mild reaction conditions (H_2O_2 oxidant, H_2O solvent, <100 °C) and in the absence of acids or toxic additives.

However, although iron was assigned as the catalytic active sites, the exact nature of these species, their evolution during the catalyst preparation procedure, and their precise role within the catalytic mechanism are not yet fully understood. Furthermore, the potential role(s) of other zeolitic functionalities, such as acidity and molecular confinement, have also not been evaluated. With these issues in mind, we aimed to definitively identify and characterize the active component(s) within commercial ZSM-5 (30), henceforth denoted as ZSM-5 $(30)_{COMM}$, and related materials for the selective oxidation of methane.

RESULTS AND DISCUSSION

Confinement Effects. It is well-known that the regular arrangement of molecular-sized pores and cavities of the framework allows zeolites to discriminate between molecules simply by size.[10] Although this feature is typically utilized in catalysis for shape selectivity,[11] it is also known that the confining nature of zeolitic micropores can also affect reaction mechanisms by directly inducing or enhancing catalytic activity.[12] This "confinement induced activity" is thought to originate from the confinement of the reacting orbitals within the zeolitic cage, essentially increasing the local concentration of the molecular orbitals within the micropores, leading to increased interactions between confined reactants and allowing unusual transition states to be accessed. Furthermore, entrapment of molecules within zeolites has also been shown to induce dipoles and multipoles, potentially strengthen or weaken some C−C bonds, and lead to modifications of the HOMO/LUMO energy levels.[13] To elucidate whether such a confinement effect is solely responsible for the catalytic activity exhibited by ZSM-5 $(30)_{COMM}$ for methane partial oxidation, silicalite-1 (i.e., heteroatom-free ZSM-5) was synthesized and tested for activity (Table 1). We note here that any material synthesized in the laboratory (i.e., any noncommercial material) is denoted with the subscript SYN.

The good agreement between the measured surface area and micropore volume for ZSM-5 $(30)_{COMM}$ and silicalite-1_{SYN} indicates that the spatial confinement within these two materials should be practically the same. From the lack of activity of silicalite-1 given in Table 1, we conclude that any confinement effect imparted by the MFI framework is not the only factor responsible for the observed activity of commercial ZSM-5. It should be noted that these materials will also differ in hydrophobicity, since framework Al^{3+} in ZSM-5 $(30)_{COMM}$ is expected to lower its hydrophobicity compared with silicalite-1_{SYN}. However, the highly active commercial ZSM-5 used thus far is still predominantly hydrophobic, and alternative Al^{3+}-containing molecular sieves of similar dimensions and acidity ($Ferrierite_{COMM}$) were also found to be much less active than

Table 1. Physical and Catalytic Properties of Commercial ZSM-5 (30) and Silicalite-1

catalyst	procedure	S_{BET}[a] ($m^2\ g^{-1}$)	V_{MICRO}[b] ($cm^3\ g^{-1}$)	product formed[c] (μmol)
ZSM-5	commercial	342	0.138	81
silicalite-1	hydrothermal	331	0.131	0
Ferrierite	commercial	380	0.144	5

[a]Surface area determined from nitrogen adsorption using the Brunauer, Emmett, and Teller (BET) equation. [b]Microporous volume determined from nitrogen adsorption isotherms using the *t*-plot method. [c]Total oxygenated product formed (MeOOH, MeOH, HCOOH, and CO_2). Reaction conditions: catalyst, various (27 mg); $P_{(CH_4)}$, 30.5 bar; $[H_2O_2]$, 0.5 M; temp, 50 °C; time, 30 min; stirring speed, 1500 rpm.

ZSM-5 $(30)_{COMM}$. Thus, the low activity observed for silicalite-1_{SYN} is due to the absence of active sites rather than a decrease in hydrophilicity inhibiting the transport of H_2O_2.

Nevertheless, it is clear that although molecular confinement alone is not responsible for catalysis, there is a clear influence of confinement on the final activity of the active catalyst, given the disparate activities between microporous materials, such as ZSM-5 $(30)_{COMM}$, and amorphous materials, such as SiO_2 or Al_2O_3, after deposition of 2.5 wt % Fe^{3+} (Supporting Information Table S1). Even between similar microporous materials, such as ZSM-5 $(30)_{COMM}$ and Ferrierite $(SiO_2/Al_2O_3 = 20)_{COMM}$ (Supporting Information Table S1), significant differences in final activity are observed at similar catalyst compositions. We will return to the potential roles of confinement on the final activity of the catalyst later.

Metal Content and Acidity. ZSM-5 is, however, not only a microporous molecular sieve but also a multifunctional material possessing both Brønsted and Lewis acidity associated with Al^{3+}. Furthermore, commercial ZSM-5 is also known to be susceptible to the presence of trace metal impurities. Indeed, elemental analysis of ZSM-5 $(30)_{COMM}$ and other related zeolites demonstrated that in addition to the expected quantities of Si and Al, all the commercial zeolites examined in this study contained trace (<500 ppm ≡ 0.05 wt %) levels of the transition metals Fe and Ti, with ZSM-5 $(30)_{COMM}$ containing 140 and 35 ppm of these metals, respectively. This is highly significant, as these metals within the MFI structure are known to be highly active oxidation catalysts. For example, TS-1 (a Ti^{4+}-containing MFI-type zeolite) is used for various selective oxidations with H_2O_2, and Fe/ZSM-5 has previously been employed for N_2O-based oxidations.[14,15] In fact, it has previously been shown that with even trace Fe concentrations (<1000 ppm), Fe/ZSM-5 is able to catalyze the one-step oxidation of benzene to phenol with N_2O.[16,17]

To investigate the role(s) of these metals, the inactive silicalite-1_{SYN} matrix was progressively doped with increasing amounts of Fe or Ti or Al by inclusion of the relevant salts during the hydrothermal synthesis procedure employed for silicalite-1. This allowed the evaluation of the role of each metal in the absence of other trace metal impurities and over a wide range of metal content. Figure 1 compares the total amount of oxygenated product (MeOOH, MeOH, HCOOH, and CO_2) produced by each catalyst as a function of a single metal species at loadings up to 1.5 wt %.

Given that the incorporation of either Ti or Al into the MFI framework at levels significantly higher than found in the commercial samples leads to only limited levels of activity, it is

dx.doi.org/10.1021/cs3007999 | ACS Catal. 2013, 3, 689−699

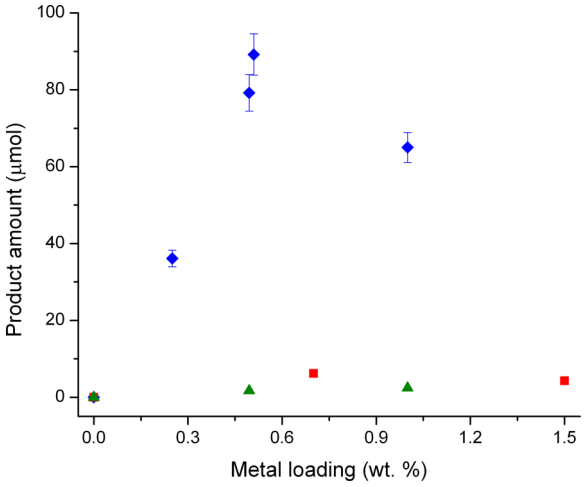

Figure 1. Catalytic activity of various MFI-type metallosilicates as a function of metal content: ▲, TS-1_{SYN} (green); ■, ZSM-5_{SYN} (Al-MFI, red); ◆, Fe-silicalite-1_{SYN} (blue). Reaction conditions: cat., various (27 mg); $P_{(CH_4)}$, 30.5 bar; [H_2O_2], 0.5 M; temp, 50 °C; time, 30 min; stirring speed, 1500 rpm.

highly unlikely that these species within the structure are those active for this challenging reaction. The low levels of activity exhibited by [Al]-MFI in the proton form over a wide Al^{3+} content also confirms that Brønsted acid sites alone are insufficient for methane oxidation catalysis and that the lack of activity previously observed for silicalite-1 (Table 1) is not due to an issue of hydrophob-/phil-icity.

In contrast, the incorporation of Fe^{3+} (Fe-silicalite-1_{SYN}) leads to a linear relationship between observed activity and Fe content up to 0.5 wt %, strongly suggesting that iron species are the active species for the reaction, although this activity decreases significantly at higher metal content. Analysis of the Al-only and Ti-only materials by ICP-OES revealed that there was also, in fact, ~25 ppm of Fe present in these samples. Using the relationship between Fe content and observed activity from the linear region of Figure 1, we would expect this level of Fe to lead to between 1 and 3 μmol of products under our standard reaction conditions. This can account for the highest level of oxygenate production observed for "Al-only" and "Ti-only" catalysts in Figure 1, and we conclude that Fe is also the essential component for catalytic activity in these materials. This observation also highlights the difficulty in preparing completely Fe-free samples of ZSM-5.

As we previously observed with ZSM-5 $(30)_{COMM}$, Fe-silicalite-1_{SYN} produces oxygenated product with a typical kinetic profile, and no induction period is observed (Supporting Information Figure S5). The primary product obtained is methyl hydroperoxide (MeOOH) (Supporting Information Figure S6), which consecutively converts to methanol (MeOH), formic acid (HCOOH), and CO_2 as the reaction proceeds. As expected in the absence of a Cu^{2+} additive, which we have shown to be necessary for the retention of MeOH at high selectivity,[7,8] the Fe-only catalyst is highly selective to HCOOH. Given the similarities in both the kinetic profile and the temporal evolution of selectivity, it is clear that Fe-silicalite-1_{SYN} is a valid model catalyst analogous to ZSM-5 $(30)_{COMM}$. We also note here that all of the oxygenated products were derived from methane, as substitution of 1/6th of the CH_4 feed with $^{13}CH_4$ led to a product distribution containing exactly 1/6 ^{13}C MeOOH, MeOH, and HCOOH.[7,8]

To further demonstrate that Fe is the key component of ZSM-5 $(30)_{COMM}$ for the selective oxidation of methane, the catalytic activity of ZSM-5 $(30)_{COMM}$ was investigated following the postsynthetic deposition of various transition metals (Figure 2). From these investigations, it is clear that, although

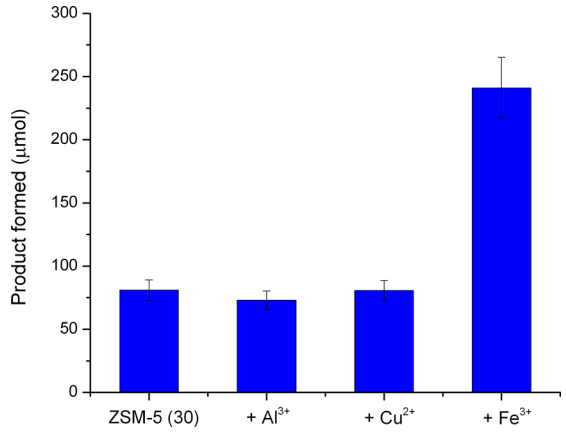

Figure 2. Catalytic activity of postsynthetically modified ZSM-5 $(30)_{COMM}$. Each metal was added at 2.5 wt % by solid state ion exchange. Reaction conditions: catalyst, various (27 mg); $P_{(CH_4)}$, 30.5 bar; [H_2O_2], 0.5 M; temp, 50 °C; time, 30 min; stirring speed, 1500 rpm.

the deposition of 2.5 wt % Al^{3+} or 2.5 wt % Cu^{2+} does not lead to any promotion of the ZSM-5 $(30)_{COMM}$ sample, deposition of 2.5 wt % Fe^{3+} leads to significant increases in catalytic activity. This is in qualitative agreement with the results obtained in Figure 1 and further confirms that Fe^{3+} species are the active sites for the reaction. However, from the relation between Fe loading and oxygenate production observed in Figure 1, we would expect the addition of 2.5 wt % Fe to lead to around 400 μmol of oxygenated product. In Figure 2 the increase in oxygenate productivity observed on addition of 2.5 wt % Fe to ZSM-5 $(30)_{COMM}$ is only around 160 μmol. This suggests that at this level of loading and with this preparation procedure, not all the Fe species are active for the reaction. This is supported by the observed decrease in activity of Fe-silicalite-1_{SYN} as the Fe content is raised above 0.5 wt %.

The normalization of activity to Fe loading allows turnover frequencies (TOFs) to be calculated (Table 2). ZSM-5 $(30)_{COMM}$, containing only 140 ppm (0.014 wt %) of impurity Fe is the most intrinsically active zeolite (Table 2). Increased concentrations of Fe, while leading to higher levels of product, exhibit lower turnover frequencies, emphasizing that at high Fe loadings, spectator species or competitive active species are also present. This is not wholly surprising, since it cannot be expected that direct framework incorporation and postsynthetic deposition methods lead to exactly the same species. Indeed, the rather poor efficiency of postsynthetic deposition methods is evident in Table 2, where the addition of substantial amounts of Fe^{3+} to the commercial material (0.5 and 2.5 wt %) leads to only marginal increases in product yield relative to the active commercial sample. In fact, by subtracting the amount of product produced by the active ZSM-5 $(30)_{COMM}$ support material, the TOFs of these materials drop by a factor of ±4−5. Furthermore, deposition of Fe^{3+} onto a laboratory-synthesized ZSM-5_{SYN} sample, which itself possesses little or no catalytic activity (Figure 1), clearly demonstrates that Fe^{3+} deposited

dx.doi.org/10.1021/cs3007999 | ACS Catal. 2013, 3, 689−699

Table 2. Catalytic Properties of Various Fe-Zeolites[a]

entry	catalyst	[Fe] (wt %)	product formed (μmol)	CO_2 selectivity[b] (%)	TOF (h^{-1})	conv (%)[c]
1	no catalyst	na	0			0.0
2	ZSM-5 $(30)_{COMM}$	0.014	81	4	2393	0.26
3	Fe-silicalite-1_{SYN}	0.5	89	6	75	0.29
4	Fe^{3+}/ZSM-5 $(30)_{COMM}$	0.5	98 (17)	10	81 (14)	0.31
5	Fe^{3+}/ZSM-5 $(30)_{COMM}$	2.5	226 (145)	12	40 (24)	0.77
6	Fe^{3+}/ZSM-5 $(40)_{SYN}$	0.5	12	*d*	10	0.04

[a]Reaction conditions: catalyst, various (27 mg); $P_{(CH_4)}$, 30.5 bar; $[H_2O_2]$, 0.5 M; temp, 50 °C; time, 30 min; stirring speed, 1500 rpm. Each catalyst was pretreated at 550 °C prior to use. [b]CO_2 selectivity calculated at iso-conversion (81 μmol product). [c]Conversion values, calculated by "total moles of product/initial moles of methane ≥ 100". Values in parentheses are the normalized yields and TOF values obtained by subtraction of the products produced by the "support" material, ZSM-5 $(30)_{COMM}$. [d]Selectivity at iso-conversion not reported due to poor activity.

postsynthetically possesses a smaller fraction of active sites (entry 6).

We note here that the conversion values achieved under these reaction conditions (Table 2) are very low (<1%). This is a consequence of the excessively high methane pressures employed in these tests to ensure that the reaction was not limited by methane availability. However, under more appropriate reaction conditions, the same catalyst(s), such as Fe-silicalite-1, were able to achieve up to a 10% methane conversion within the same time scale, as described elsewhere.[7]

The Fe content of a particular catalyst also has a profound effect on the observed C-based selectivity (Table 2). Although a decrease in partial oxygenate selectivity (i.e., oxygenated products not including CO_2) may be expected at higher levels of conversion, comparing the catalytic activity of 2.5 wt % Fe^{3+}/ZSM-5 $(30)_{COMM}$ to ZSM-5 $(30)_{COMM}$ at isoconversion demonstrates that the addition of large quantities (2.5 wt %) of Fe^{3+} to ZSM-5 $(30)_{COMM}$ significantly enhances the overoxidation process, as the selectivity to CO_2 increases from 4% to 12% at a fixed oxygenate level of 81 μmol. Therefore, although the further deposition of 2.5 wt % Fe^{3+} clearly results in the formation of more active sites, a significant proportion of the deposited metal is in a form active for the overoxidation process. Furthermore, large quantities of Fe^{3+} were also highly detrimental to the H_2O_2-based selectivity of the catalysts: although a corrected[18] H_2O_2/product stoichiometry of 2:1 was obtained for the commercial material (170 μmol H_2O_2 required for 81 μmol product), the reaction stoichiometry of 2.5 wt % Fe/ZSM-5 $(30)_{COMM}$ was significantly higher, with 4110 μmol H_2O_2 consumed for only 241 μmol of product (stoichiometry of 18:1). This indicates that most of the H_2O_2 is lost to unproductive side reactions when using materials with high Fe content. We note that the full product distributions of these catalysts are provided in the Supporting Information (Table S2).

It is clear, therefore, that significant effort should be devoted to the identification of which Fe species are responsible for high reactivity and selectivity and which are active for the competitive overoxidation process, active for H_2O_2 decomposition, or are completely inactive. Thus, it is vital to determine the number, geometry, valence state, and nuclearity of the Fe sites present in these materials and the effect of the Fe loading on the population of each. Furthermore, the effect of thermal pretreatment (found to be necessary for activity[7]) on each of these factors will be important.

Although the most intrinsically active material based on iron loading is ZSM-5 $(30)_{COMM}$ (Table 2), the extremely low levels of Fe within this sample make spectroscopic investigations hugely difficult. Furthermore, it cannot be excluded at this stage that other features of this commercial sample, such as Brønsted acid sites, may be noncatalytic promoters of the Fe-catalyzed reaction. In fact, the significantly higher TOFs of ZSM-5 $(30)_{COMM}$ versus Fe-silicalite-1_{SYN} suggests that the additional features of this material do enhance its activity. In contrast, although 2.5 wt % Fe^{3+}/ZSM-5 $(30)_{COMM}$ produced significantly more oxygenated product than commercial ZSM-5 (30) alone, the decreased selectivity and TOF of this system (due to the formation of spectator and competing active sites), coupled with the simultaneous presence of the active sites present in ZSM-5 $(30)_{COMM}$ itself, ensures that this material is also not the most suitable for the partial oxidation of methane. Thus, to achieve the most accurate and best-quality interpretations, initial spectroscopic and catalytic studies focused on Fe-silicalite-1_{SYN}, containing *only* Fe at a loading of ≤0.5 wt %.

Identification of the As-Prepared Iron Species. FT-IR spectroscopy has previously been found to be a useful tool for following the isomorphous substitution of framework Si^{4+} species by various transition metals (e.g., Fe^{3+}, Ti^{4+}).[19,20] In fact, it has previously been reported that a well-defined fingerprint region stretch exists at a wavenumber of ∼700 cm^{-1} for the Si−O−Fe bond formed upon isomorphous substitution of Fe^{3+} in zeolite frameworks.[17] Accordingly, the inclusion of Fe^{3+} in the silicalite-1 structure following hydrothermal synthesis of Fe-silicalite-1_{SYN} is supported by the FT-IR spectrum presented in Figure 3: the as-synthesized Fe-silicalite-1_{SYN} contains a band at ∼710 cm^{-1} that is clearly absent in the Fe-free analogue (silicalite-1). In addition, the weak absorbance at 965 cm^{-1} may also indicate isomorphous framework substitution. Previously, such an absorbance has been attributed to an Si−O−Ti vibration in TS-1.[20] However, it has also been proposed that this absorbance is related to an Si−

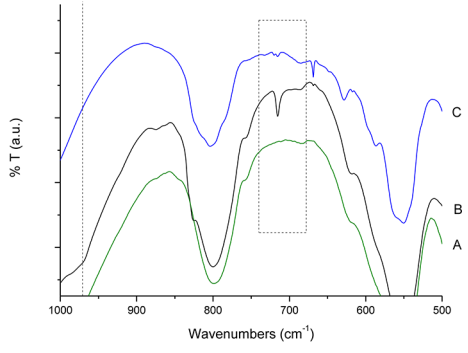

Figure 3. FT-IR spectra for (green/A) silicalite-1_{SYN} and (black/B) 0.5 wt % Fe-silicalite-1_{SYN} (as synthesized) and (blue/C) 0.5 wt % Fe-silicalite-1_{SYN} (after removal of organic template).[7].

dx.doi.org/10.1021/cs3007999 | ACS Catal. 2013, 3, 689−699

O^- species, formed by perturbation of the silicalite-1 framework upon incorporation of a suitable transition metal.[21] In fact, other framework-substituted zeolites, such as Ta-silicalite-1, have also been shown to contain this absorbance.[20,22] It appears, then, that the best interpretation is that the 710 cm^{-1} band is a direct indication of Fe framework substitution, whereas the 965 cm^{-1} feature indicates that this is accompanied by some disruption of the local structure, again suggesting isomorphous substituion. The lack of vibrational modes between 700 and 600 cm^{-1} in the as-synthesized material (Figure 3, black/B), typically attributed to extraframework Fe species, also indicates that most if not all of the Fe present in the sample is located in the T-sites of the zeolite framework.[19] However, the low Fe concentrations utilized and the poor sensitivity of the FT-IR technique make it difficult to place a quantitative limit on the level of extraframework Fe present and the degree of successful isomorphous substitution achieved.

A much more conclusive indication of the nature of the Fe species within the as-synthesized Fe-silicalite-1_{SYN} was provided through UV−vis spectroscopy. Though d−d transitions in Fe-containing zeolites are both spin- and symmetry-forbidden,[23] the position and intensity of the $Fe^{3+} \leftarrow O$ charge-transfer bands provides information on the coordination and agglomeration of Fe within the sample, through the deconvolution of the spectra into relevant subbands.[24−27] The first band (observed between 200 and 250 nm) is attributed to isolated Fe^{3+} species located within the zeolite framework.[25] In contrast, absorbances between 250 and 350 nm are associated with those of isolated or oligonuclear extraframework Fe species within the micropores.[26] At absorbances between 350 and 450 nm, the deconvoluted bands are attributed to larger Fe_xO_y clusters.[23] Finally, bands observed at wavelengths ≥450 nm originate from agglomerated iron oxide species, present on the external surface of the zeolite.[24,25] Although it is possible to quantitatively differentiate among the wide range of Fe species within zeolites by deconvolution of the absorbance spectra into subbands, it should be noted that the exact values of each molar extinction coefficient are unknown, although they have been shown to be of the same order of magnitude.[25] Thus, UV−vis analysis provides a semiquantitative overview of the various Fe species present in the sample.

In the as-synthesized sample (Figure 4, A), it is clear that the Fe species are well dispersed and incorporated into the T-sites of the zeolitic framework, given the narrow (fwhm ∼ 60 nm), well-defined absorbances at 210 and 240 nm. The lack of any shoulders above ∼250 nm confirms the absence of extraframework or (bulk) iron oxides in the sample. This demonstrates the success of the synthesis procedure: although the facile precipitation of iron hydroxides and oxides during the formation of the zeolite gel is well-known to inhibit framework incorporation, the utilization of oxalic acid clearly prevents this process, probably due to prior complexation of Fe^{3+}.

From these observations, it can be concluded that in the synthesis of Fe-silicalite-1_{SYN}, Fe has successfully been incorporated into the MFI framework, in full agreement with the FT-IR analysis. Together with XRD patterns (Figure 5), electron microscopy[7] and the porosity measurements, it can be concluded that MFI-type Fe-silicalite-1_{SYN} has, indeed, been synthesized and contains only isomorphously substituted framework Fe^{3+} species in the as-synthesized form.

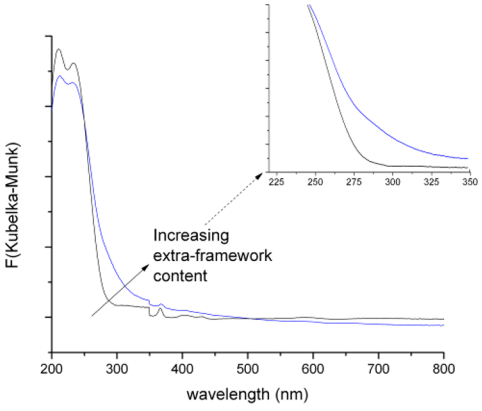

Figure 4. UV−vis spectra for 0.5 wt % Fe-silicalite-1_{SYN} (black/A) as synthesized and (blue/B) after removal of organic template.

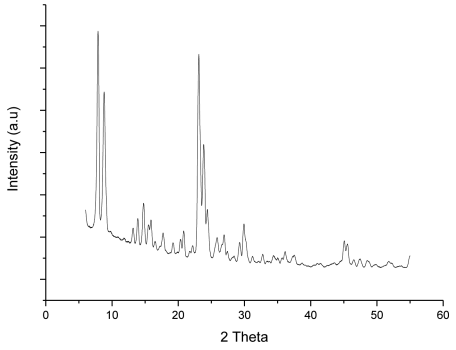

Figure 5. XRD pattern for Fe-silicalite-1_{SYN} after removal of organic template. The pattern is consistent with an MFI-type zeolite. Porosymmetry measurements determined that the material has a total surface area of 330 m^2 g^{-1} and a micropore volume of 0.13 g cm^{-3}.

Evolution of the Iron Species upon Heat Pretreatment. We have noted that FT-IR and UV−vis spectra for the as-synthesized Fe-silicalite-1_{SYN} are consistent with a homogeneous distribution of framework Fe^{3+}. However, the complete synthesis procedure for Fe-silicalite-1 and related materials involves two high-temperature treatments, as displayed in Scheme 1. The first is required to remove the residual organic template from the zeolite pores. Following ion exchange with NH_4NO_3, a second thermal treatment yields the acidic (i.e. H-

Scheme 1. Activation Procedures Employed for Fe-Silicalite-1[a]

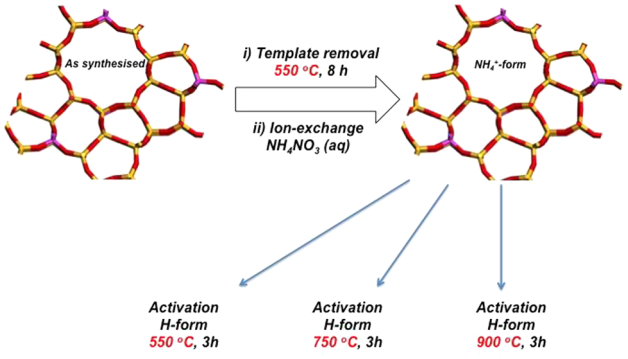

[a]Removal of the template at 550 °C, followed by ion-exchange, leads to an NH_4-form zeolite. Further activation (≥550 °C) yields the final catalyst.

dx.doi.org/10.1021/cs3007999 | ACS Catal. 2013, 3, 689−699

form of the zeolite). Although our investigations herein (Figure 1) have demonstrated that Brønsted acid sites are not responsible for catalytic activity, previous work[7] on this system has revealed that high-temperature (>400 °C) pretreatment of NH_4-ZSM-5 $(30)_{COMM}$ was required to attain the highest levels of activity. Thus, the effect of thermal pretreatment on the nature of the Fe species within the catalyst must be considered.

Marked changes in the aforementioned FT-IR and UV−vis spectra are, indeed, observed when the first high-temperature thermal treatment, required for removal of the residual organic template, is carried out (Figures 3C and 4B). This is indicative of significant changes in the coordination state and agglomeration of Fe^{3+} species within the material. Following this removal of the template (and conversion to the NH_4-form), it is clear that a decrease in the absorbances at 210 and 240 nm of the UV−vis spectrum are observed, along with an increase in absorbances between 250 and 350 nm. This indicates that Fe has at least partially migrated from the zeolite framework, as contributions to the spectra at these wavelengths are associated with extraframework Fe species of isolated or oligonuclear nature within the micropores.[26] In addition, the very minor absorbances observed between 350 and 450 nm, which are attributed to larger Fe clusters, indicate a clustering process that can occur only following extraction of Fe from the zeolite framework. Despite some inherent limitations—namely, the slight differences in extinction coefficients between various Fe species and the high number of absorbance bands within a short wavelength range—deconvoluting the overlapping bands associated with each Fe species provides a (semi)quantitative overview over the extent of this migration. As expected from the relatively narrow absorbance spectrum for NH_4−Fe-silicalite-1_{SYN}, deconvolution suggests that only a minor part of the Fe has migrated to the extraframework and that a large percentage of Fe^{3+} (71.3%) is still located within the zeolite framework (Supporting Information, Table S3).

Similar conclusions can be drawn from the FT-IR spectrum of NH_4−Fe-silicalite-1_{SYN} (Figure 3C). This clearly demonstrates that following the removal of the residual organic template, the intensity of the Fe−O−Si stretch decreases significantly. Concurrently, new stretches in the region between 700 and 600 cm^{-1} are observed, and these have been attributed previously to extraframework Fe_xO_y-type clusters within/on the zeolite and to iron oxide-type species.[19] This again indicates that Fe is removed from the framework of the zeolite during the high-temperature treatment required to remove the organic template. The observed change in coordination for the Fe centers on migration to the extraframework sites leads to coordination of the metal center by water ligands, which can be exchanged for reactant molecules more easily than the lattice oxygen of the framework.[15] It is important to add that the relatively poor stability of Fe^{3+} in the framework of ZSM-5 has previously been reported by, for example, Berlier et al., who observed that it was almost impossible to remove the organic template from the micropores of ZSM-5 without affecting the coordination environment of Fe.[28,29] Extensive migration of Fe upon removal of the organic template has also been observed by Perez-Ramirez and the group of Zecchina.[23,30−32]

Given that thermal pretreatment of NH_4-ZSM-5 $(30)_{COMM}$ was previously found to lead to significant increases in catalytic activity,[7] it can be hypothesized that migration of Fe^{3+} from the zeolitic framework is a prerequisite for activity. This would also agree with the observation that the postsynthetic deposition of Fe can also enhance catalytic activity; typically, postsynthetic methods are unable to place transition metal ions into the zeolite framework. To probe this hypothesis further, the catalytic activity of NH_4−Fe-silicalite-1_{SYN} was investigated to determine the effect of framework Fe^{3+} removal in the absence of a second high-temperature treatment, that is, without full conversion to the H-form.

In view of the significant activity observed for the NH_4-form Fe-silicalite-1_{SYN} sample (Table 3, entry 1), it is clear that extraframework Fe species formed through migration of Fe from the framework upon high-temperature treatment are highly active for the oxidation of methane. Furthermore, it is clear that a highly active catalyst can be formed without the additional high-temperature activation step typically performed on zeolitic materials (Scheme 1) for conversion to the H-form, again confirming that Brønsted acid sites are not required for activity. Nevertheless, given the effectiveness of high-temperature pretreatment on the observed catalytic activity of both Fe-silicalite-1_{SYN} and ZSM-5 $(30)_{COMM}$,[7,8] further pretreatment of the NH_4-form Fe-silicalite-1_{SYN} was performed. Although these pretreatments will result in the conversion of the material to the H-form, it has been conclusively demonstrated that this is not responsible for the observed catalytic activity and that the subsequent changes in Fe speciation are significantly more relevant.

Table 3. Catalytic Activities of Various Fe-Containing MFI-Type Zeolites[a]

entry	catalyst	product formed (μmol)
1	NH_4−Fe-silicalite-1_{SYN}	75
2	silicalite-1_{SYN}	0
3	2.5 wt % Fe_2O_3/silicalite-1_{SYN}	0

[a]Reaction conditions: catalyst, various (27 mg); $P_{(CH_4)}$, 30.5 bar; $[H_2O_2]$, 0.5 M; temp, 50 °C; time, 30 min; stirring speed, 1500 rpm.

From the UV−vis spectra presented in Figure 6, it is clear that by adding a second thermal pretreatment to the Fe-silicalite-1, significant increases in the extraction of framework Fe^{3+} are achieved. Indeed, though a second 550 °C pretreatment achieves only minor additional framework removal, unsurprising as template removal is also performed at 550 °C, increasing the pretreatment temperature to 750 °C leads to

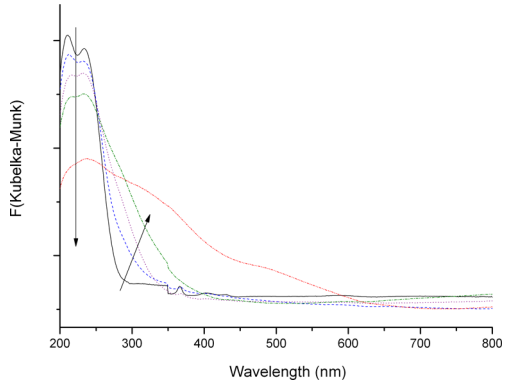

Figure 6. UV−vis spectra for 0.5 wt % Fe-silicalite-1_{SYN} at various stages of pretreatment: (black/solid) as synthesized, (blue/dashed) after removal of organic template and conversion to NH_4-form, (purple/dotts) calcined 550 °C, (green/dash-dot) calcined 750 °C, and (red/dash-dot-dot) calcined 900 °C. Part of the data are previously reported in the Supporting Information of reference 7.

dx.doi.org/10.1021/cs3007999 | ACS Catal. 2013, 3, 689−699

significant additional migration of Fe^{3+} from the framework. In particular, the absorbances at 210 and 240 nm are only around one-half as intense as the as-synthesized material, and absorbances at wavelengths up to ~350 nm are observed. Indeed, absorbances at 250−350 nm (attributable to extraframework Fe in the micropores) now represent the major component of the spectra. Pretreatment at 900 °C induces even greater migration, and significant contributions are thus also observed from larger clusters (350−450 nm) and even from bulk iron oxide species (≥450 nm), presumably on the external surface of the zeolite. In fact, after treatment at 900 °C, bulk Fe oxide accounts for almost 20% of the total Fe species in Fe-silicalite-1_{SYN} pretreated at 900 °C, in good agreement with its brown/orange color. The full deconvolution data of each UV−vis spectrum is provided (Supporting Information, Table S3).

The catalytic activity of each of these samples was subsequently investigated (Figure 7). Although the presence

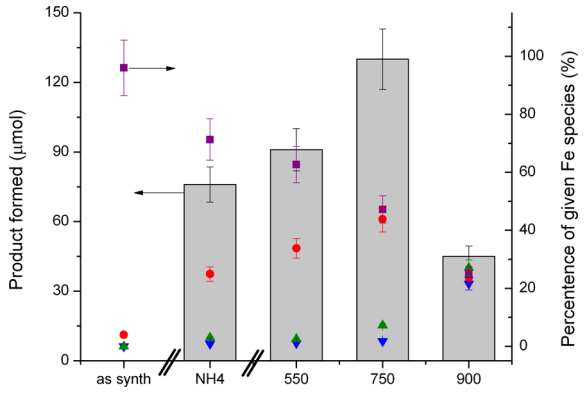

Figure 7. Comparison of the amount of oxygenated products produced for reactions using Fe-silicalite-1_{SYN} catalysts after different thermal pretreatments. The NH_4-form precursor is also illustrated for comparison. Reaction conditions: catalyst, various (27 mg); $P_{(CH_4)}$, 30.5 bar; $[H_2O_2]$, 0.5 M; temp, 50 °C; time, 30 min; stirring speed, 1500 rpm. The deconvoluted UV−vis data are also provided as scatter points. Key: squares, isolated, tetrahedral framework Fe; circles, extraframework Fe within the micropores; up triangles, larger Fe clusters; down triangles, bulk Fe oxides.

of the template prohibits a fair comparison of activity for the as-synthesized sample, the data clearly show that by increasing the temperature of the thermal pretreatment of NH_4−Fe-silicalite-1_{SYN} beyond that required for template removal, significant increases in the observed activity can be obtained. It is clear that the most active sample is that pretreated at 750 °C, which is around 30% more active than the sample pretreated at 550 °C. In each case, a similar product distribution was achieved, with CO_2 accounting for <10% of the total products (Supporting Information, Table S4); however, excessive thermal pretreatment at 900 °C is clearly detrimental to activity, which drops by around 70% relative to the optimum 750 °C material. It should be noted that XRD analysis confirmed that the MFI structure was maintained after each of the pretreatments, although some very minor loss of crystallinity was observed after pretreatment at 900 °C.

By overlaying the deconvoluted UV−vis data (Supporting Information, Table S3) and catalytic activity, it is immediately clear that there is a positive correlation between the percentage of extraframework Fe species in the micropores of Fe-silicalite-1_{SYN} and catalytic activity. Indeed, by plotting the percentage of these species against catalytic activity, a positive straight line relationship with an R^2 value >0.92 is obtained (Supporting Information, Figure S7). This not only agrees favorably with the extraction of Fe from the zeolite framework but also significantly strengthens the hypothesis that extraframework Fe species within the micropores are those active for the reaction.

We stress here that this positive correlation between the amount of extraframework species within the micropores of Fe-silicalite-1_{SYN} and catalytic activity is in full agreement with our previous investigations on ZSM-5 $(30)_{COMM}$.[7] In this instance, XANES analysis demonstrated a positive correlation between a decreasing pre-edge feature (related to an Fe 1s−3d transition) and catalytic activity.[7] In this case, the pre-edge transition arises from the mixing of the 3d and 4p orbitals of the transition metal ion. This mixing has been shown to be 0% for Fe in an octahedral geometry (i.e., no mixing), and 7.5% for Fe in tetrahedral geometry.[33] Thus, the decreasing pre-edge feature is an indication of decreasing tetrahedral content and suggests that activity is related to an increase in extraframework Fe species in ZSM-5 $(30)_{COMM}$, in full agreement with our investigations presented here. Furthermore, initial EXAFS analysis revealed that in the most active commercial samples (ZSM-5 $(30)_{COMM}$ calcined or steamed at 600 °C), the average Fe−Fe coordination was between 1.0 and 2.5, which is again consistent with an extraframework Fe species within the zeolite micropores, possessing between 2 and 4 Fe atoms (Supporting Information, Table S5).[7] Subsequent DFT calculations were performed and demonstrated that the best fit between theory and EXAFS data could be obtained for an extraframework binuclear species, $Fe_2(\mu_2\text{-}OH)_2(OH)_2(H_2O)_2]^{2+}$. Although the broadness of typical UV−vis bands makes it almost impossible to identify the exact number of Fe atoms in the active species found within Fe-silicalite-1, spatial confinements of the MFI framework suggest that such species would not contain more than 3−4 Fe atoms.

It is notable that if pretreatment is performed under more severe conditions (900 °C), a significant decrease in activity is observed. This is seen to correspond to the formation of bulk iron oxide species and indicates that such species, formed through either excessive thermal pretreatment of Fe-silicalite-1_{SYN} or the deposition of Fe^{3+} by postsynthesis treatments, lead to inactive Fe species for methane oxidation. Indeed, the inactivity of such species was clearly exemplified by testing a mechanical mixture of α-Fe_2O_3/silicalite-1 (Table 3, entry 3): even at large Fe loadings (≤2.5 wt %), this material was incapable of activating methane under the reaction conditions employed.

Even so, α-Fe_2O_3 (and catalysts containing large quantities of α-Fe_2O_3) was found to lead to large increases in H_2O_2 decomposition and CO_x selectivity. For example, Fe-silicalite-1 pretreated at 900 °C, which contains ±20% bulk Fe oxide (Supporting Information, Table S3), consumed over 30% more H_2O_2 and had a CO_2 selectivity 50% higher than the sample pretreated at 750 °C (containing only 1.3% bulk iron oxide), despite the 60% decrease in activity (Supporting Information, Table S4). It is likely that this nonselective H_2O_2 decomposition by iron oxide accounts for the much poorer activity of the catalyst pretreated at 900 °C relative to the samples pretreated at 550 or 750 °C. Even accounting for its lower percentage of active species (i.e., its lower percentage of extraframework Fe species within the micropores, Supporting Information Table S3), Fe-silicalite-1_{SYN} pretreated at 900 °C

dx.doi.org/10.1021/cs3007999 | ACS Catal. 2013, 3, 689−699

appears to be less active than predicted by the straight line plot. It is likely that excessive H_2O_2 decomposition due to bulk iron oxide leads to a decreased rate of oxidation, given the first-order relationship between the catalytic rate and H_2O_2 concentration.[7]

It appears, then, that controlled formation of extraframework oligomeric Fe species is a prerequisite for obtaining both high catalytic activity and high carbon- and hydrogen-based selectivity. These results thus explain the poorer selectivity of the 2.5 wt % Fe^{3+}/ZSM-5 $(30)_{COMM}$ catalyst prepared by postsynthetic deposition (Table 2, entries 4−6) and the poorer activity of Fe-silicalite-1_{SYN} at higher Fe content (Figure 1). It can be expected that higher Fe content, a similar pretreatment will produce a greater fraction of bulk iron oxide and a smaller fraction of oligonuclear Fe species, thus leading to poorer activity and selectivity.

Comparison to N_2O-Based Systems. In the reactions reported here with Fe containing microporous materials, there is a clear relationship between the evolution of extraframework Fe oligomers and catalytic activity for the low-temperature partial oxidation of methane in aqueous H_2O_2. The oxidation of benzene to phenol and the oxidation of methane to a chemisorbed methoxy species have also been reported over Fe-containing zeolites, although in the gas phase and in a two step, noncatalytic process using N_2O as an oxygen source. Extraction of framework Fe^{3+} within these systems also appears to be a prerequisite for catalytic activity.[15,34−36] However, the two systems appear to be quite distinct. First, it is well-known that N_2O-based systems require (auto)reduction of Fe^{3+} to Fe^{2+} for oxidation to occur, with this reduction being facilitated by (i) a high-temperature pretreatment at temperatures >800 °C and (ii) a subsequent thermal treatment above 550 °C in vacuo or an inert atmosphere (typically helium). The necessity for such an aggressive treatment has been attributed to various factors, but stems from the inability of Fe^{3+} to coordinate N_2O and subsequently form surface-adsorbed reactive oxygen species.[15] These pretreatments thus facilitate the (auto)-reduction of Fe^{3+} to Fe^{2+}, the key active site for N_2O-based oxidations.[15]

In contrast, XANES measurements of the active catalytic materials discussed here consistently show a pre-edge feature at ±7115 eV (Figure 8a−g), which is absent from the same spectra for FeO (Figure 8h). In addition, no shift in the edge positions was observed following heat treatment, as would be expected for a reduction of Fe^{3+} to Fe^{2+}. These features demonstrate that only Fe^{3+} is present within the active catalytic materials, precluding the possibility that H_2O_2 is simply replacing N_2O as an oxidant. In the aqueous low-temperature reactions reported here, an alternative active species must be formed to facilitate the selective and catalytic partial oxidation of methane. However, we note that XANES is a technique that provides only an average insight into the Fe species within these materials. Thus, to experimentally verify that N_2O, or, indeed, α-oxygen, is not a suitable oxidant for the catalysis reported here, the catalytic activity of Fe-silicalite-1_{SYN} was monitored following high-temperature treatment in helium; importantly, such pretreatment conditions were found to be highly detrimental to catalytic activity (Supporting Information, Table S6). This is in good agreement with the lower activity of Fe-silicalite-1_{SYN} after pretreatment at 900 °C and further suggests that distinct Fe-based chemistry is observed in this system.

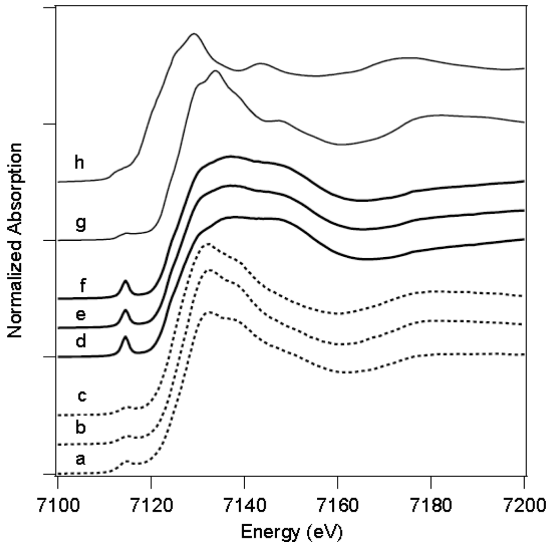

Figure 8. XANES analysis on a series of ZSM-5 $(30)_{COMM}$ samples, containing 140 ppm of Fe as impurity, and Fe-silicalite-1_{SYN} samples, containing 0.5 wt % Fe, after various pretreatment conditions: (a) ZSM-5 $(30)_{COMM}$, NH_4-form, uncalcined; (b) ZSM-5 $(30)_{COMM}$, calcined at 600 °C; (c) ZSM-5 $(30)_{COMM}$, steamed at 600 °C; (d) Fe-silicalite-1_{SYN}, NH_4-form, (e) Fe-silicalite-1_{SYN} calcined, 550 °C; (f) Fe-silicalite-1_{SYN}, steamed, 550 °C, along with Fe reference standards for (g) Fe^{3+} in Fe_2O_3, and (h) Fe^{2+}, FeO.

Further to this, samples of ZSM-5 $(30)_{COMM}$, 2.5 wt % Fe^{3+}/ZSM-5 $(30)_{COMM}$ and Fe-silicalite-1_{SYN} were also pretreated with N_2O according to the reported literature procedures and tested for catalytic activity, in the absence of H_2O_2. Although only stoichiometric quantities of product could theoretically be obtained, the complete inactivity of these samples in the absence of H_2O_2 further demonstrates that Fe^{2+}/N_2O-based chemistry is not a suitable method for performing selective methane oxidation in the aqueous phase and within a closed catalytic cycle, as is known from the literature (Supporting Information, Table S6).

Catalytic Robustness and Heterogeneity. Although significant progress has been made in the identification of both the selective and nonselective forms of Fe, forming a stable, reusable and truly heterogeneous catalyst is one of the greatest challenges within the field of liquid phase oxidation.[37] To verify that the developed catalytic system satisfies this criteria, a hot-filtration test of Fe-silicalite-1_{SYN} was initially performed so as to test if any Fe^{3+} species leached into the reaction solution have catalytic activity. After filtering off the solid material in this way, the oxidation reaction completely ceased, clearly demonstrating the heterogeneous nature of this catalyst (Supporting Information, Figure S5). Figure 9 also shows that Fe-silicalite-1 is a stable catalyst for methane oxidation that can be reused without loss of yield over five full recharges of the reactor. It is notable that no chemical or thermal treatments were required to maintain these levels of activity; the catalysts were simply filtered from the aqueous solution and dried at ambient temperature for 24 h prior to reuse.

In addition to catalytic studies, ICP measurements also confirmed that the Fe loading in Fe-silicalite-1 (0.5 wt %) remained constant, even after five repeat reactions, suggesting that no detectable leaching of Fe into the aqueous phase takes place during the reaction (Supporting Information, Table S7).

dx.doi.org/10.1021/cs3007999 | ACS Catal. 2013, 3, 689−699

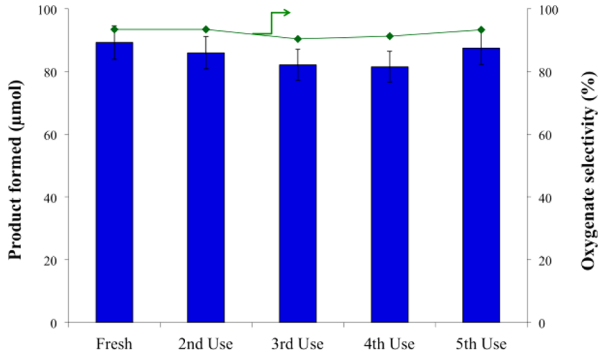

Figure 9. Reusability studies of Fe-silicalite-1. Reaction conditions: catalyst, Fe-silicalite-1 (27 mg); $P_{(CH_4)}$, 30.5 bar; $[H_2O_2]$, 0.5 M; temp, 50 °C; time, 30 min; stirring speed, 1500 rpm.

Atomic Absorption and ICP studies of the reaction filtrate also demonstrated a lack of Fe, confirming that the amount of Fe leached from the catalyst (if any) is below the detectability limit of these techniques. From these experiments, it can be confirmed that Fe-silicalite-1 is an active, selective, stable, and truly heterogeneous catalyst for the selective oxidation of methane.

CONCLUSIONS

It has been shown that the catalytic activity of commercial ZSM-5 (30) and related MFI-type zeolites for the selective oxidation of methane is related to the presence of oligomeric Fe species within the micropores. Although effectively formed through postsynthetic deposition of Fe^{3+}, extraction of Fe^{3+} from the zeolitic framework sites prior to reaction by high-temperature pretreatment is a more effective method of forming highly active catalysts. Optimal activity and selectivity (with respect to both carbon and hydrogen) is obtained following pretreatment of Fe-silicalite-1 at 750 °C, which ensures the maximum percentage of the oligonuclear Fe species, which have been shown to be the likely active species. Excessive thermal pretreatment at 900 °C, however, leads to the formation of bulk iron oxide, which, although unable to activate methane, leads to excessive H_2O_2 decomposition and CO_x formation. In addition to significant levels of activity and selectivity, the so-formed catalytic materials are also highly stable and may be used for multiple repeat reactions without loss of activity or metal content. Nevertheless, having now identified the key active component within these materials for the selective oxidation of methane, some interesting questions remain unanswered.

The first concerns the influence of confinement on the activity of the catalysts (Supporting Information, Table 2). Having identified extraframework Fe species within the micropores as being the active component of the catalyst, we hereby propose that the effect of confinement is not related to a molecular confinement effect increasing the local concentration of the reactants, but that confinement of the active site within the micropores enhances its activity for the reaction. In support of this, we note that we have previously identified a high-energy, high-spin $[Fe^{IV}{=}O]^{2+}$ species as being the key C−H activating component of the catalyst through DFT calculations.[7] Key work in the literature has proposed that the confinement of metal cations within microporous structures leads to a more facile formation of, and a stabilization of, such high-energy species.[38] It is therefore possible that in non-microporous materials, such as SiO_2, the key high-spin $[Fe^{IV}{=}O]^{2+}$ species cannot be formed as efficiently. Although such an effect cannot fully explain the curious influence of the specific microporous structure and explain why other zeolites such as Ferrierite are so much less active, we can postulate that depending on the precise framework topology, the electronic and steric factors required to facilitate the formation of the key active site are not identical.

Another unanswered question concerns the disparate activity per Fe site exhibited by the Fe-only and Fe-silicalite-1_{SYN} samples examined here and Fe- and Al-containing analogues, such as commercial ZSM-5. Although we have ruled out the possibility that Al^{3+} possesses a catalytic role, it is clear that other factors are at play in the commercial sample that account for its higher activity per Fe site. We note that such a noncatalytic promotional role has previously been observed for other Fe-zeolite-catalyzed processes, such as NO_x decomposition. In these cases, it has been proposed that the increased levels of activity per Fe site, in the simultaneous presence of Al, is related to a dispersion of the active Fe species on specific sites associated with framework Al^{3+}.[15] Since we have identified extraframework isolated or oligonuclear Fe species as being the active component of the catalyst, an increased dispersion of Fe would certainly account for higher activity per Fe site due to a decrease in unwanted clustering and a decreased formation of bulk Fe oxide. Nevertheless, the exact reasons for this promotion are topics of ongoing research and will form the basis of a future publication.

EXPERIMENTAL SECTION

Catalyst Synthesis. MFI-type zeolites containing various amounts of Fe and Al were prepared by hydrothermal synthesis, according to a procedure adapted from reference 39. An example procedure for Fe-silicalite-1 is provided. Tetraethylorthosilicate (Sigma Aldrich, 99.999% trace metal basis) was added dropwise to a solution of tetrapropylammonium hydroxide (Sigma Aldrich, 20 wt % in water) and homogenized at 60 °C for 3 h. Concurrently, a solution containing iron nitrate (Sigma Aldrich, 98%) and oxalic acid was prepared and subsequently added to the TEOS/TPAOH solution after 3 h. The gel was homogenized for 16 h at 60 °C prior to crystallization in a Teflon-lined, stainless steel autoclave at 175 °C for 120 h. Where required, sodium aluminate (Sigma Aldrich, 50−55 wt % Al_2O_3) was used as the Al precursor. TS-1 was prepared according to the original method of Tarramasso et al.[40] Commercial NH_4−ZSM-5 (SiO_2/Al_2O_3 = 30) was obtained from commercial sources (Zeolyst) and was activated prior to use, typically by calcination at 550 °C for 3 h. Where appropriate, Fe^{3+}, Cu^{2+}, or Al^{3+} were also deposited onto commercial ZSM-5 (30) by solid state ion exchange, an illustrative procedure of which is provided. A 2.5 wt % portion of Fe^{3+}/ZSM-5 $(30)_{COMM}$ was prepared by grinding the appropriate amount of acetylacetonate precursor with the required amount of NH_4−ZSM-5 $(30)_{COMM}$. After mechanical grinding for 15 min, the resultant solid was calcined at 550 °C for 3 h in a flow of air.

Catalyst Pretreatment. Samples synthesized by hydrothermal synthesis were first treated at 550 °C (1 °C min^{-1}) for 8 h (5 h N_2, 3 h air) to remove the organic template. A 3-fold ion exchange with NH_4NO_3 (1 M, 90 °C, 3 × 8 h) subsequently yielded the NH_4-form precursor. NH_4-form samples of Fe-silicalite-1 and ZSM-5 were subsequently heat

dx.doi.org/10.1021/cs3007999 | ACS Catal. 2013, 3, 689−699

treated, that is, activated/converted to the H-form by a second pretreatment, performed at various temperatures.

Catalyst Characterization. Powder X-ray diffraction was performed using a PANalytical X'PertPRO X-ray diffractometer, with a Cu Kα radiation source (40 kV and 40 mA). Diffraction patterns were recorded between 6 and 55° 2θ at a step size of 0.0167° (time/step =150 s, total time =1 h). FT-IR spectroscopy was performed by forming self-supporting wafers from a small amount of sample and KBr. The spectra were recorded on a Jasco FT-IR660 Plus over a range of 4000−400 cm^{-1} at a resolution of 2 cm^{-1}. UV−vis analysis was performed on an Agilent Cary 4000 UV−visible spectrophotometer equipped with diffuse reflectance setup. Samples were scanned between 190 and 900 nm at a scan rate of 600 nm min^{-1}. Na, Si, and Al contents were determined by neutron activation analysis (NAA). Metal contents were determined by ICP-OES to an accuracy of ±10%.

Kinetic Evaluation. Catalytic evaluation was carried out in a 50 mL stainless steel autoclave containing a Teflon liner vessel (working volume, 35 mL). The vessel was charged with an aqueous solution of H_2O_2 (10 mL, 0.5 M, 5000 μmol), and the desired amount of catalyst (typically 27 mg). After evacuation of contaminant gases, the autoclave was heated to the reaction temperature (typically 50 °C) and vigorously stirred at 1500 rpm once the desired temperature was obtained. The vessel was cooled in ice (12 °C) following the appropriate reaction time, and the resultant solution was filtered and analyzed.

Analytical Methods. Liquid products were identified through ^1H NMR spectroscopy on a Bruker 500 MHz Ultra-Shield NMR spectrometer and quantified against a 1 vol % TMS/$CDCl_3$ internal standard, previously calibrated against authentic standards. Detectability limits of <0.1 μmol were achieved. End H_2O_2 concentrations were determined by titration against acidified $Ce(SO_4)_2$ solution. Gaseous phase products were quantified by means of an FID-GC (Varian 450-GC) fitted with a CP-Sil 5CB capillary column (50m length, 0.32 mm i.d.). The GC was equipped with a methanizer unit, and CO_2 was quantified against a calibration curve constructed from commercial standards (BOC).

Definitions. Partial oxygenates; methyl hydroperoxide (CH_3OOH), methanol (CH_3OH) and formic acid (HCOOH). Total product formed; partial oxygenates + CO_2.

Oxygenate selectivity:

$$\frac{\text{moles (partial oxygenates)}}{\text{moles (total oxygenated product)}} \times 100$$

Turnover frequency: moles (partial oxygenated species formed) mol^{-1} (Fe) h^{-1}.

■ ASSOCIATED CONTENT

Ⓢ Supporting Information

Additional experimental data and analysis results as noted in text. This material is available free of charge via the Internet at http://pubs.acs.org.

■ AUTHOR INFORMATION

Corresponding Author

*E-mail: ceri.hammond@chem.ethz.ch; hutch@cardiff.ac.uk.

Present Addresses

[⊥]Department of Chemistry and Applied Biosciences, ETH Zürich, Wolfgang-Pauli-Strasse 10, CH-8093 Zürich, Switzerland

[‖]University College London, 20 Gordon Street, WC1H 0AJ London, U.K., and Research Complex at Harwell, Rutherford Appleton Laboratory, Harwell Oxford, Didcot, OX11 0FA U.K.

[¶]Stephenson Institute for Renewable Energy, Chemistry Department, The University of Liverpool, Crown Street, Liverpool, L69 7ZD U.K.

Notes

The authors declare no competing financial interest.

■ ACKNOWLEDGMENTS

This work formed part of the Methane Challenge. The Dow Chemical Company is thanked for their financial support. Computing facilities for this work were provided by ARCCA at Cardiff University, HPC Wales, and the UK's HPC Materials Chemistry Consortium (MCC). The MCC is funded by EPSRC (EP/F067496). Portions of this work were performed at the DuPont-Northwestern-Dow Collaborative Access Team (DND-CAT) located at Sector 5 of the Advanced Photon Source (APS). DND-CAT is supported by E.I. DuPont de Nemours & Co., The Dow Chemical Company, and Northwestern University. Use of the APS, an Office of Science User Facility operated for the U.S. Department of Energy (DOE) Office of Science by Argonne National Laboratory, was supported by the U.S. DOE under Contract No. DE-AC02-06CH11357.

■ REFERENCES

(1) Hammond, C.; Conrad, S.; Hermans, I. *ChemSusChem* **2012**, *5*, 1668−1686.

(2) Golisz, S. R.; Gunnoe, T. B.; Goddard, W. A., III.; Groves, J. T.; Periana, R. A. *Catal. Lett.* **2011**, *141* (2), 213−221.

(3) Hammer, G.; Lubcke, T.; Kettner, R.; Pillarella, M. R.; Recknagel, H.; Commichau, A.; Neumann, H.-J.; Paczynska-Lahme, B. Natural Gas. *Ullmann's Encyclopaedia of Industrial Chemistry*; Wiley-VCH: Weinheim, 2006; Vol. *23*; pp 739−792.

(4) Abbasi, T.; Tauseef, S. M.; Abbasi, S. A. *Renewable Sustainable Energy Rev.* **2012**, *16* (5), 3228−3242.

(5) Fiedler, E.; Grossmann, G.; Keresbohm, D. B.; Weiss, G.; Witte, C. Methanol. *Ullmann's Encyclopaedia of Industrial Chemistry*; Wiley-VCH: Weinheim, 2011; Vol. *23*; pp 26−48.

(6) Chang, C. D.; Silvestri, A. J. *J. Catal.* **1977**, *47* (2), 249−259.

(7) Hammond, C.; Forde, M. M.; Ab Rahim, M. H.; Thetford, A.; He, Q.; Jenkins, R. L.; Dimitratos, N.; Lopez-Sanchez, J. A.; Dummer, N. F.; Murphy, D. M.; Carley, A. F.; Taylor, S. H.; Willock, D. J.; Stangland, E. E.; Kang, J.; Hagen, H.; Kiely, C. J.; Hutchings, G. J. *Angew. Chem., Int. Ed.* **2012**, *51* (21), 5129−5133.

(8) Hammond, C.; Jenkins, R. L.; Dimitratos, N.; Lopez-Sanchez, J. A.; Ab Rahim, M. H.; Forde, M. M.; Thetford, A.; Murphy, D. M.; Stangland, E. E.; Hagen, H.; Moulijn, J. M.; Taylor, S. H.; Willock, D. J.; Hutchings, G. J. *Chem.—Eur. J.* **2012**, *18*, 15735−15745.

(9) For consistency with our previous work (see refs 7, 8), where we use both Cu and Fe in the final catalyst, we have retained the catalyst description as Cu/Fe/ZSM-5, since it is only during this paper that we conclusively demonstrate the nature of the species that catalyze the reaction and that it is the Fe species alone that are responsible for the observed catalysis.

(10) McBain, J. W. *Trans. Faraday Soc.* **1932**, *28*, 0408−0409.

(11) Weisz, P. B. *Pure Appl. Chem.* **1980**, *52* (9), 2091−2103.

(12) Sastre, G.; Corma, A. *J. Mol. Catal A: Chem.* **2009**, *305* (1−2), 3−7.

(13) Corma, A.; Garcia, H.; Sastre, G.; Viruela, P. M. *J. Phys. Chem. B* **1997**, *101* (23), 4575−4582.

(14) Cavani, F.; Teles, J. H. *ChemSusChem* **2009**, *2* (6), 508−534.
(15) Zecchina, A.; Rivallan, M.; Berlier, G.; Lamberti, C.; Ricchiardi, G. *Phys. Chem. Chem. Phys.* **2007**, *9* (27), 3483−3499.
(16) Yuranov, I.; Bulushev, D. A.; Renken, A.; Kiwi-Minsker, L. *J. Catal.* **2004**, *227* (1), 138−147.
(17) Wen, B.; Chen, L. X.; Sachtler, W. M. H. *Catal. Lett.* **2002**, *82* (1−2), 7−11.
(18) To determine the true amount of H_2O_2 utilized during the reaction, the loss of H_2O_2 through only thermal decomposition was monitored and subtracted from the total amount of H_2O_2 consumed during a typical reaction under identical conditions.
(19) Ratnasamy, P.; Kumar, R. *Catal. Today* **1991**, *9* (4), 329−416.
(20) Fan, W.; Duan, R.-G.; Yokoi, T.; Wu, P.; Kubota, Y.; Tatsumi, T. *J. Am. Chem. Soc.* **2008**, *130* (31), 10150−10164.
(21) Ziolek, M.; Nowak, I. *Catal. Today* **2003**, *78* (1−4), 543−553.
(22) Ko, Y. S.; Ahn, W. S. *Microporous Mesoporous Mater.* **1999**, *30* (2−3), 283−291.
(23) Perez-Ramirez, J.; Groen, J. C.; Bruckner, A.; Kumar, M. S.; Bentrup, U.; Debbagh, M. N.; Villaescusa, L. A. *J. Catal.* **2005**, *232* (2), 318−334.
(24) Kumar, A. S.; Perez-Ramirez, J.; Debbagh, M. N.; Smarsly, B.; Bentrup, U.; Bruckner, A. *Appl. Catal., B* **2006**, *62* (3−4), 244−254.
(25) Perez-Ramirez, J.; Kumar, M. S.; Bruckner, A. *J. Catal.* **2004**, *223* (1), 13−27.
(26) Hensen, E. J. M.; Zhu, Q.; Janssen, R. A. J.; Magusin, P.; Kooyman, P. J.; van Santen, R. A. *J. Catal.* **2005**, *233* (1), 123−135.
(27) Hensen, E. J. M.; Zhu, Q.; Hendrix, M.; Overweg, A. R.; Kooyman, P. J.; Sychev, M. V.; van Santen, R. A. *J. Catal.* **2004**, *221* (2), 560−574.
(28) Berlier, G.; Spoto, G.; Bordiga, S.; Ricchiardi, G.; Fisicaro, P.; Zecchina, A.; Rossetti, I.; Selli, E.; Forni, L.; Giamello, E.; Lamberti, C. *J. Catal.* **2002**, *208* (1), 64−82.
(29) Ferretti, A. M.; Oliva, C.; Forni, L.; Berlier, G.; Zecchina, A.; Lamberti, C. *J. Catal.* **2002**, *208* (1), 83−88.
(30) Bordiga, S.; Buzzoni, R.; Geobaldo, F.; Lamberti, C.; Giamello, E.; Zecchina, A.; Leofanti, G.; Petrini, G.; Tozzola, G.; Vlaic, G. *J. Catal.* **1996**, *158* (2), 486−501.
(31) Berlier, G.; Spoto, G.; Fisicaro, P.; Bordiga, S.; Zecchina, A.; Giamello, E.; Lamberti, C. *Microchem. J.* **2002**, *71* (2−3), 101−116.
(32) Zecchina, A.; Bordiga, S.; Spoto, G.; Damin, A.; Berlier, G.; Bonino, F.; Prestipino, C.; Lamberti, C. *Top. Catal.* **2002**, *21* (1−3), 67−78.
(33) Heijboer, W. M.; Glatzel, P.; Sawant, K. R.; Lobo, R. F.; Bergmann, U.; Barrea, R. A.; Koningsberger, D. C.; Weckhuysen, B. M.; de Groot, F. M. F. *J. Phys. Chem. B* **2004**, *108*, 10002−10012.
(34) Panov, G. I.; Sobolev, V. I.; Dubkov, K. A.; Parmon, V. N.; Ovanesyan, N. S.; Shilov, A. E.; Shteinman, A. A. *React. Kinet. Catal. Lett.* **1997**, *61* (2), 251−258.
(35) Wood, B. R.; Reimer, J. A.; Bell, A. T.; Janicke, M. T.; Ott, K. C. *J. Catal.* **2004**, *225*, 300−306.
(36) Knops-Gerrits, P. P.; Goddard, W. A., III. *J. Mol. Catal A: Chem.* **2001**, *66* (1), 135−145.
(37) Sheldon, R. A.; Wallau, M.; Arends, I.; Schuchardt, U. *Acc. Chem. Res.* **1998**, *31* (8), 485−493.
(38) Yumura, T.; Takeuchi, M.; Kobayashi, H.; Kuroda, Y. *Inorg. Chem.* **2009**, *48*, 508−517.
(39) Prikhod'ko, R. V.; Astrelin, I. M.; Sychev, M. V.; Hensen, E. J. M. *Russ. J. Appl.d Chem.* **2006**, *79*, 1115−119.
(40) Taramasso, M.; Perego, G.; Notari, B. Preparation of porous crystalline synthetic material comprised of silicon and titanium oxides. U.S. Patent 4410501, 1982.